Hydrogen Exchange of Primary Amide Protons in Basic Pancreatic Trypsin Inhibitor: Evidence for NH_2 Group Rotation in Buried Asparagine Side Chains†

Erik Tüchsen*,‡ and Clare Woodward§

Roskilde University, DK-4000 Roskilde, Denmark, and Department of Biochemistry, University of Minnesota, St. Paul, Minnesota 55108

Received May 13, 1987; Revised Manuscript Received July 21, 1987

ABSTRACT: Hydrogen–deuterium exchange is measured for the buried primary amide groups of Asn-43 and Asn-44 in bovine pancreatic trypsin inhibitor. Amide protons trans and cis to the amide carbonyl oxygen (H_E and H_Z, respectively) exchange at indistinguishable rates. Uncorrelated exchange of H_E and H_Z is established for both residues by following the nuclear Overhauser enhancement from H_E to H_Z during the deuterium exchange. The exchange of Asn-43 and Asn-44 side-chain protons differs qualitatively from exchange of primary amide groups in fully solvated model compounds, for which H_E generally exchanges faster than H_Z. The equal rates for the buried primary amide H_E and H_Z in BPTI are not a consequence of coupled exchange. The data indicate rapid rotation around the CO–NH_2 bond for both Asn-43 and Asn-44 and suggest considerable lability of intramolecular hydrogen bonds. The side chain of Asn-43 has all of its polar atoms integrated into the very stable hydrogen-bonded structure of the protein. Asn-44 is hydrogen-bonded to side chains and to a buried water molecule. Solvent isotope exchange is several orders of magnitude more restricted by protein secondary and tertiary structure than the CO–NH_2 rotation, indicating that $N^{\delta}H_2$ groups flip many times before hydrogen isotope exchange occurs.

The buried primary amide groups of Asn-43 and Asn-44 in BPTI[1] have interesting local environments in the folded protein. All polar atoms of both groups participate in hydrogen bonds, the $N^{\delta}H_2$ group donating two and C=O accepting one. Asn-44 H_Z (cis) makes an unusual H bond with the π-electron cloud of the Tyr-35 aromatic ring from which it experiences a very large ring current magnetic deshielding (Tüchsen & Woodward, 1987a).[2] Asn-44 H_E (trans) donates a hydrogen bond to an internal water molecule, and O accepts a hydrogen bond from the side chain of Arg-20. All of these are relatively mobile parts of the protein structure. The Asn-43 primary amide group, on the other hand, is H-bonded to main-chain polar atoms in the most rigid parts of the molecule. Asn-43 donates two H bonds to the main-chain carbonyl groups of Tyr-23 and of Glu-7 and accepts one from Tyr-23 peptide NH.

We have recently assigned the NMR resonances of primary amide hydrogen atoms of BPTI Asn-44, and the main-chain NH of Gly-37, and specifically assigned resonances of H_Z and H_E for both Asn-43 and Asn-44 (Tüchsen & Woodward, 1987a). Here we report the hydrogen isotope exchange kinetics for the buried primary amide groups, which reflect the dynamics of their local environments in the BPTI solution structure.

Accurate determination of isotope exchange rates for a proton in the protein depends on spectral resolution of the proton line from lines of other exchangeable protons. The buried primary amide proton resonances in BPTI may be resolved from overlapping peptide amide proton resonances by specific ^1H labeling utilizing pH-dependent differences in exchange kinetics. Standard two-dimensional NMR techniques are less useful for observation of primary amide than peptide amide proton exchange as no cross-peaks are formed with nonexchangeable protons in correlated spectra. For fully solvated primary amide model compounds, acid-catalyzed exchange rate constants are 10–100-fold larger than those for peptide amide model compounds, while base-catalyzed exchange rate constants are similar (Molday et al., 1972; Perrin et al., 1981; Perrin & Johnston, 1981). Consequently, the cross-over point between acid- and base-catalyzed exchange, pH_{min}, is usually 1–2 pH units higher for primary amide protons than for the peptide NH's. Although the protein folding results in a considerable spread of pH_{min}s for peptide amide protons, pH_{min}s for the buried primary amide protons remain higher than those for peptide protons.

Conclusions concerning BPTI conformational dynamics rely on comparison of protein and fully solvated model compound isotope exchange kinetics. In primary amide model compounds, rotation around the CO–NH_2 bond is relatively slow compared with the rate of proton exchange. Individual exchange rates can therefore be obtained for H_E and H_Z. In general, H_E of model compounds exchanges faster than H_Z. Since the mechanism for acid-catalyzed exchange involves a tetrahedral N-protonated intermediate with possibility of $-NH_3^+$ rotation, the ratio of exchange rate constants is smaller for acid-catalyzed exchange, $r = k(H_E)/k(H_Z) = 1$–2, than for base-catalyzed exchange (r = 2–8). For acetamide in water, r is 1.2 and 7.5 for acid- and base-catalyzed exchange, respectively (Perrin & Johnston, 1981; Perrin et al., 1981). Similar differences have been found for Asn and Gln side-chain protons in small peptides (Krishna et al., 1979; Narutis & Kopple, 1983).

† Supported by NIH Grant 26242 and a grant from the Danish Natural Sciences Research Council.

‡ Roskilde University.

§ University of Minnesota.

[1] Abbreviations: BPTI, basic pancreatic trypsin inhibitor (bovine); FT, Fourier transform; FID, free induction decay; NOE, nuclear Overhauser enhancement; NMR, nuclear magnetic resonance; ppm, parts per million; IR, infrared spectroscopy.

[2] Erratum: There is an error in our previous paper (Tüchsen & Woodward, 1987a). The tick marks on the abscissa of Figure 9 are erroneously labeled 8.5, 8.0, 7.5, 3.5, and 3.0 ppm. The numbers should be 8.0, 7.9, 7.8, 3.4, and 3.3 ppm, respectively.

0006-2960/87/0426-8073$01.50/0

Table I: Exchange Rate Constants, k, of Buried Primary Amide Protons

	Asn-44				Asn-43		
pH	H_E[a]	H_Z[a]	H_Z NOE[b]	pH	H_E[a]	H_Z[a]	H_Z NOE[b]
1.5	33 (11%)			1.0	0.33 (8%)		
2.1	11.0 (5%)	11.2 (2%)		1.0	0.27 (32%)	0.46 (12%)	
2.5	2.7 (3%)			1.5	0.06 (60%)	0.11 (15%)	
2.6	2.4 (8%)	2.6 (5%)	5.1 (11%)	2.0	0.044 (12%)	0.042 (14%)	
3.0	0.48 (17%)			2.5	0.020 (26%)	0.018 (50%)	
4.0	0.19 (6%)			7.5	0.09 (9%)	0.11 (3%)	
4.5	0.24 (7%)			8.5	0.78 (8%)		
4.5	0.10 (14%)			8.55	1.0 (9%)	0.86 (9%)	
5.1	0.18 (9%)			8.6	1.4 (8%)		3.7 (13%)
5.5	0.37 (8%)	0.30 (20%)		10.0	29 (7%)	32 (6%)	
5.8	0.65 (10%)						
5.9	0.59 (8%)	0.58 (10%)					
6.0	0.52 (6%)		1.5 (6%)				
6.2	1.1 (9%)	0.93 (7%)	2.6 (5%)				
6.6	1.5 (10%)						
7.0	6.2 (4%)						
k_H[c]		1.1 (8%)				3.7×10^{-3} (9%)	
k_{OH}[c]		5.4×10^5 (13%)				2.7×10^3 (40%)	
pH_{min}		4.6				4.5	

[a] Pseudo-first-order rate constants ($\times 10^{-3}$ min^{-1}) (standard error). [b] Decay rate constant for NOE difference peak. For both residues the NOE is measured for H_Z while H_E is kept saturated. [c] Second-order catalytic constants (M^{-1} min^{-1}) obtained by a balanced least-squares fit of data in the table to the equation $k = k_H[H^+] + k_{OH}K_W/[H^+]$; $K_W = 10^{-14.9}$ M^2.

For the buried primary amide protons in BPTI, we find that (1) observed exchange rates are identical for both protons on the same N and (2) their exchange is uncorrelated. This indicates that rapid rotation about the C–N bond occurs while the primary amide group is buried and without solvent contact.

Materials and Methods

Samples described in the present paper contain 1.5–3 mM BPTI (Aprotinin, Novo; Novo Industries, Copenhagen, lot 32-65 or 3007-85) in 0.3 M KCl. Values of pH are direct meter readings calibrated by standard commercial buffers at pH 7.00 and 4.00. FT NMR spectra are measured at 300 MHz (Nicolet 300 NMR) or 250 MHz (Bruker AC250).

The use of ^1H labeling procedures to sort out specific groups of exchangeable proton resonances in the NMR spectrum has been described (Tüchsen & Woodward, 1985a, 1987a,b; Tüchsen et al., 1987). Specific ^1H labeling of the Asn-44 primary amide protons and the preparation of samples for studying the Asn-43 primary amide protons are described in Tüchsen and Woodward (1987a). Samples selectively labeled with ^1H at Asn-43 $N^\delta H_2$ were prepared by first labeling all exchangeable sites with ^2H by heating the protein to 90 °C in ^2H_2O at pH 5. The protein was then transferred to ^1H_2O at pH 1.0 and exchanged for 15 h at 40 °C for ^1H labeling of Asn-43 $N^\delta H_2$ while the slow β-core protons of peptide NH's including Asn-24 NH remain ^2H labeled. Finally, the sample was freeze-dried and then redissolved in ^2H_2O at high pH. A large number of peptide NH's exchange >10-fold faster than Asn-43 $N^\delta H_2$ and immediately exchange ^1H for ^2H, and Asn-43 primary amide resonances can be observed without overlap from these.

NOE difference spectra were obtained as described by Wagner (1980). In this method, two FID's are collected simultaneously in adjacent blocks of memory; in one of these, NOE's are generated by a selective low-intensity continuous irradiation for 0.7 s while in the other spectrum the irradiation frequency is shifted 10 ppm downfield outside the spectral region. NOE difference spectra were routinely collected in 2×4000 double-precision data points and each FID was the sum of 5000–6000 transients.

Rates of hydrogen exchange were obtained by measuring peak intensity vs time in a series of FT spectra. Exchange rates from the time series of NOE pairs are obtained from peak intensities measured in the off resonance irradiated spectra. Pseudo-first-order rate constants are determined from nonlinear least-squares fits of an exponential rate equation to experimental data, and standard errors are estimated from the scatter of the data points.

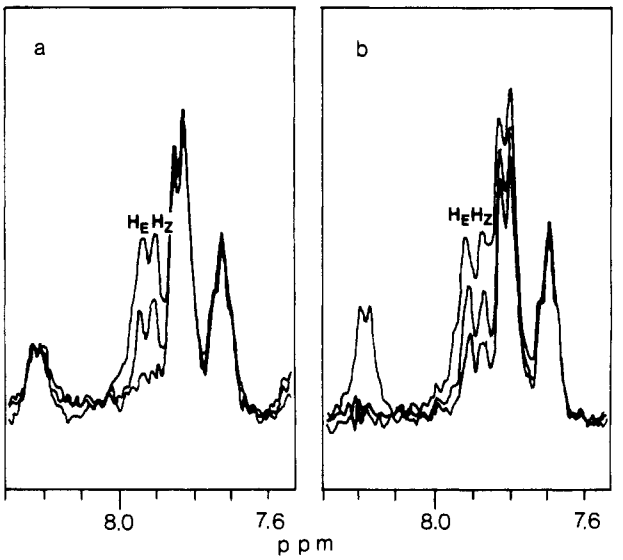

FIGURE 1: Direct comparison of exchange of Asn-43 H_Z and H_E atoms. (a) Acid-catalyzed exchange. The sample containing 10 mg of BPTI in 0.5 mL of ^2H_2O–0.3 M KCl was first incubated at pH 8.5 for 30 min to exchange out overlapping resonances. Then, pH was adjusted to 1.0, and spectra were recorded after incubation at 25 °C for 10 min, 26 h, and 90 h, respectively. (b) Base-catalyzed exchange. A solution containing 20 mg of BPTI/mL of 0.3 M KCl–^2H_2O at pH 7.6 was incubated at 25 °C. The spectra are obtained for separate 0.5-mL aliquots after pH adjustment to 1.5. The exchange times are 10 min, 66 h, and 144 h, respectively. The spectra are obtained at 300 MHz, 25 °C, and resolution enhanced by weighting the FIDs with a "double-exponential" function (Nicolet).

Results

H_E and H_Z Exchange Rates. The H_E and H_Z protons of the buried Asn side chains in BPTI exchange isotope with solvent at indistinguishable rates, given in Table I. The close similarity of H_E and H_Z rates is illustrated for Asn-43 in Figures 1 and 2 and for Asn-44 in Figure 3.

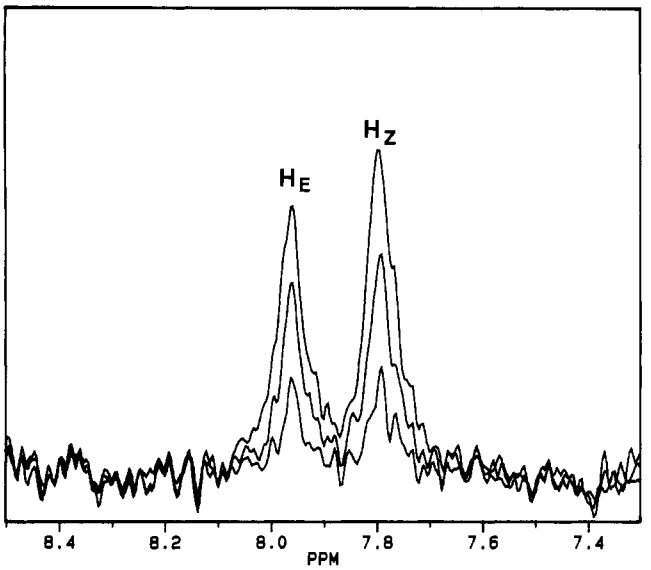

FIGURE 2: Exchange of Asn-43 $N^{\delta}H_2$ at pH 10, 25 °C. The spectra are difference spectra obtained by subtracting a spectrum collected after 80 min (four half-lives) of exchange. Accumulation time for each spectrum is 10 min starting at 5, 25, and 45 min after the final pH adjustment. Interference of Asn-43 H_Z with Asn-24 NH at 7.8 ppm is minimized by selective isotope labeling as described under Materials and Methods.

The stacked spectra in Figure 1 are measured at low pH where Asn-43 H_E and H_Z are both resolved and their resonance intensities can be directly compared. The experiment in Figure 1a shows acid-catalyzed exchange. The sample is exchanged at pH 1.0 in an NMR sample tube incubated in a water bath at 25 °C, and spectra are recorded at intervals over 4 days. The doublet-like appearance of the peaks around 7.9 ppm, with equal intensities of the two peaks, is maintained throughout, indicating identical exchange rates for H_E and H_Z.

Base-catalyzed exchange of Asn-43 H_E and H_Z may be similarly compared by inspection of Figure 1b. As for acid-catalyzed exchange, the two resonances maintain similar intensities during the base-catalyzed exchange. Individual traces in Figure 1b are spectra of aliquots withdrawn from a larger volume of BPTI maintained at pH 7.6 in a thermostated bath and adjusted to pH 1.5. The spectra are recorded at pH 1.5 rather than pH 7.5–8.6 because at pH >3 Asn-43 H_Z overlaps the nonexchangeable Tyr-35 $C^{\epsilon}H$ doublet at 7.8 ppm and the peptide NH of Asn-24, which exchanges at a rate very similar to that of the Asn-43 side-chain protons.

The scalar coupling between Asn-43 H_E and H_Z is very small and usually unresolved. Occasionally, a coupling of ca. 4 Hz was resolved for Asn-43 H_Z (e.g., lower trace in Figure 1b) and less often for both protons. When the coupling is resolved for both peaks, intensities follow an AX pattern with relatively increased intensities of the central half of both doublets. These occasional splittings have a small adverse effect on the accuracy of the rate determination.

Base-catalyzed exchange for Asn-43 H_E and H_Z at high pH was measured for a sample exchanging in the NMR probe. This is possible when obstructive overlaps are eliminated by selective isotope labeling and difference spectroscopy (Figure 2). Spectra in Figure 2 are recorded under conditions of relatively fast base-catalyzed exchange at pH 10. As at lower pH, exchange rates for H_E and H_Z are identical within error. Differential labeling of Asn-43 H_Z and Asn-24 NH is feasible at acidic pH where the Asn-43 side-chain protons exchange severalfold faster than the Asn-24 main-chain NH. A slightly increased intensity of the Asn-43 H_Z resonance relative to that of H_E, Figure 2, is a consequence of fractional Asn-24 NH

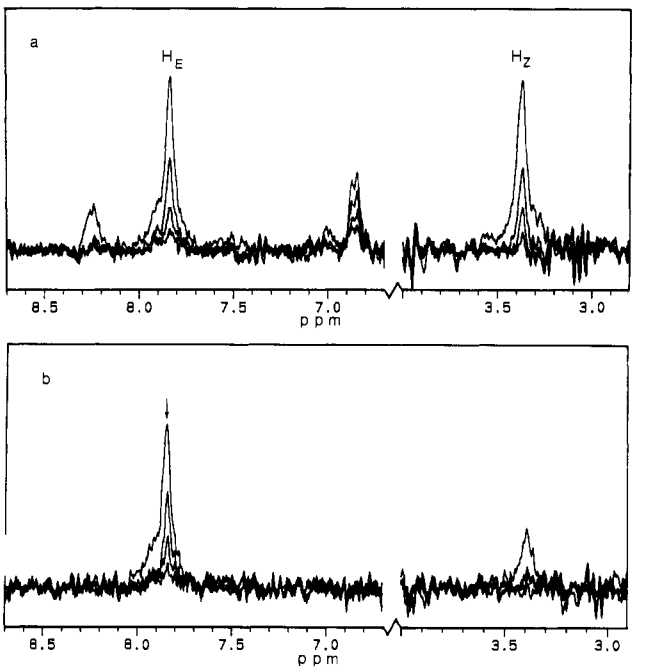

FIGURE 3: Comparison of exchange of Asn-44 H_Z and H_E atoms. (a) Exchange difference spectra at pH 2.1 showing acid-catalyzed exchange. Individual spectra are recorded at 1-h intervals, and the substracted spectrum is recorded after eight exchange half-lives. (b) NOE exchange difference showing NOE difference peaks from exchangeable protons only. NOE exchange difference spectra (Tüchsen & Woodward, 1987a) are obtained by subtracting from the spectra in (a) simultaneously accumulated spectra in which Asn-44 H_E is saturated for 0.7 s prior to the measuring pulse. The Asn-44 primary amide protons were specifically ^1H labeled by exchanging fully deuteriated protein in ^1H_2O at pH 1.5 for 30 min and reexchanging other labile protons with ^2H in ^2H_2O at pH 4.5 for 2 h.

^1H labeling. Satisfactory accuracy of the exchange rate is obtained by following the full course of the decay as in Figure 2.

Comparison of Asn-44 H_Z and H_E acid-catalyzed exchange is shown in Figure 3a. Because H_Z is overlapped with nonexchangeable resonances at 3.4 ppm, the spectra in Figure 3a, like those in Figure 2, are exchange difference spectra obtained by subtraction of the spectrum of fully deuteriated BPTI from a time series of spectra of the exchanging sample. Since Asn-44 H_E and H_Z resonances are resolved by specific labeling, interference from overlapping exchangeable resonances is minimized. Their rate constants, given in Table I, may therefore be measured at all pHs while the sample exchanges in the NMR probe. As for Asn-43 primary amide protons, the Asn-44 protons exchange at indistinguishable rates both by acid and base catalysis (Figure 3a and Table I).

Correlation of H_Z and H_E Exchange. As suggested by Wagner (1980), the correlation of exchange of two labile protons can be assessed by comparing their exchange rates with decay rates for the mutual NOE between the protons [see also Boelens et al. (1985) and Roder et al. (1985a,b)]. While the resonance peak intensity monitors directly the ^1H content of that site, the NOE difference peak is proportional to the fraction of molecules with both sites ^1H labeled. If both H's exchange simultaneously, then the relative NOE is expected to remain constant, and the decay rate of the NOE difference peak is expected to equal the exchange rates for both protons. If, instead, the two protons exchange randomly, then the NOE difference peak should decay twice as fast as either of the proton resonances.

NOE decay rates, given in Table I, are about twice the exchange rates for H_E and H_Z, indicating uncorrelated ex-

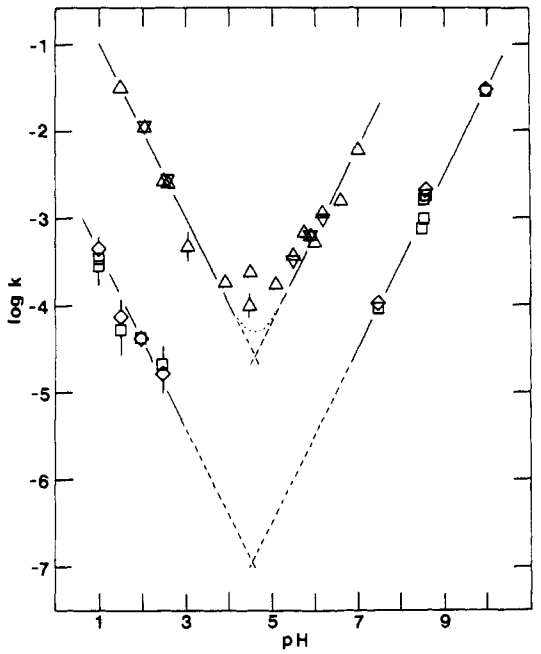

FIGURE 4: Log exchange rate constant (min^{-1}) vs pH for Asn-43 and Asn-44 side-chain protons. Exchange rates are at 25 °C: (△) Asn-44 H_E; (▽) Asn-44 H_Z; (□) Asn-43 H_E; (◇) Asn-43 H_Z. The dotted line shows the expected curve shape for Asn-44 without contributing uncatalyzed exchange.

change. The NOE decay rates are taken from experiments as illustrated in Figure 3b and in Figure 4 of Tüchsen and Woodward (1987a), in which the low-field H_E is saturated and the NOE is detected for H_Z.

For acid-catalyzed exchange the decay rate of the NOE for Asn-44 is, within error, 2 times the exchange rate for each of the protons, indicating complete lack of correlation. The measurement is not feasible for Asn-43 at low pH because of the partial overlap of H_E and H_Z resonances. For base-catalyzed exchange, a slightly faster decay of the NOE difference peak than expected for uncorrelated exchange may be significant for both residues. It indicates negative cooperativity and could be due to an isotope effect on the chemical exchange. A similar effect might be expected for acid-catalyzed exchange but is not observed. Base-catalyzed exchange relies on formation of a hydrogen bond between NH and catalyst. Since ^2H is less electrophilic than ^1H, then the N–^1H bond polarization and exchange rate may be decreased by a geminal ^2H. This deviation is opposite to the effect expected for correlated hydrogen exchange.

pH Dependence of Exchange. Exchange rate constants for primary amide protons are plotted as a function of pH in Figure 4. The data for both Asn-43 and Asn-44 indicate first-order acid and base catalysis at pHs >1.5 units from pH_{min}. However, for Asn-44 the shape of the curve through the minimum is more shallow than expected for a simple sum of two first-order rate terms. This can be taken to indicate a significant contribution of uncatalyzed direct exchange with water (Tüchsen et al., 1987). From the present data and data of Richarz et al. (1979), it can be concluded that any contribution of uncatalyzed exchange for Asn-43 would be at least 10^3-fold less than that for Asn-44. Interestingly, Asn-44 H_E is hydrogen bonded to one of the buried waters, Wat-113, in BPTI (Tüchsen et al., 1987; Wlodawer et al., 1984). A contribution from uncatalyzed exchange to the overall exchange near pH_{min} is in line with a similar trend for peptide amide protons H bonded to buried water molecules (Tüchsen et al., 1987). The exchange kinetics of small primary amides are in many cases heavily influenced by uncatalyzed direct exchange with solvent in the region of pH_{min} (Krishna et al., 1982; Redfield & Waelder, 1979; Kakuda & Mueller, 1974).

Base-catalyzed exchange rates for Asn-43 H_E and H_Z in Table I are in excellent agreement with rates obtained for Asn-43 H_E by Richarz et al. (1979), whereas rates for acid-catalyzed exchange in Table I are roughly 10-fold larger than rates given by these authors. Rates for Asn-43 H_Z and for both Asn-44 protons have not previously been reported.

Values of pH_{min}, 4.5 and 4.6 for Asn-43 and Asn-44, respectively, are obtained by extrapolation to the intersection point of the unit slope acid- and base-catalyzed branches of the curves in Figure 4. These are similar to pH_{min} of model compounds. In a study on *N*-acetylasparagine N^{α}-methylamide (Asn′) in ^1H_2O, Krishna et al. (1982) find pH_{min} 4.5 and 4.8 for H_E and H_Z, respectively (pH measured in ^1H_2O). These values are also reproduced in oligopeptides (Narutis & Kopple, 1983). The primary amide protons of poly(DL-asparagine), measured by a tritium tracer technique, have pH_{min} 4.5 at 0 °C (Molday et al., 1972).

The slowing of the exchange of the buried Asn side-chain protons in BPTI may be estimated by comparing values of k_H and k_{OH} with corresponding values for Asn′, taken as averages for H_E and H_Z. Then, quenching factors for acid- and base-catalyzed exchange are $10^{-7.1}$ and $10^{-6.1}$ for Asn-43 and $10^{-4.7}$ and $10^{-3.8}$ for Asn-44, respectively. The paradox of similar pH_{min} and unequal quenching factors for acid- and base-catalyzed exchange is a consequence of the different ionization constants for ^1H_2O and ^2H_2O, 10^{-14} and $10^{-14.9}$, respectively.

Discussion

In BPTI, the buried primary amide H_E and H_Z protons exchange at indistinguishable rates. This is in contrast to small model compounds (Krishna et al., 1982; Perrin et al., 1981; Redfield & Waelder, 1979) and oligopeptides (Narutis & Kopple, 1983; Krishna et al., 1979), in which H_E consistently exchanges faster than H_Z. Exchange of primary amide protons in model compounds is measured by fast methods, such as transfer of solvent saturation, with a time scale of milliseconds to seconds. In this time frame, rotation around the C–N bond is restricted due to its double-bond character, and consequently, there is little mixing of H_E and H_Z protons.

The similarity of the exchange rates for H_E and H_Z of the buried primary amide groups observed here is most likely a consequence of rotation around the C–N bond, which averages the isotopic contents in the H_E and H_Z positions on the time scale of these experiments. The observed exchange rates, then, are averages of the exchange rates from the two positions. An alternative potential explanation is that both protons bound to a given N atom exchange simultaneously upon transient solvent access in a single conformational fluctuation. This possibility, however, is amply ruled out by the observed lack of correlation of H_E and H_Z exchange.

Rotational rate constants for small primary amide compounds in aqueous solution are in the range 1–10 s^{-1} (Redfield & Waelder, 1979). For propionamide, k_{rot} = 5 s^{-1} (Tropp & Redfield, 1980). Rotational rate constants for amides in ethylene glycol and other solvents, given by Perrin et al. (1981) and Perrin and Johnston (1981), indicate little solvent effect on the rotation. Their rates are generally less than those measured by Redfield and co-workers. For our estimates, we use k_{rot} = 1 s^{-1}.

For the isotopic averaging to be efficient in the protein k_{rot} must be larger than the largest exchange rate constant observed. That is, k_{rot} must be >0.03 and >0.006 min^{-1} for

Asn-43 and Asn-44, respectively. An upper limit for the factor by which C–N rotation is quenched by folding the primary amide group into the protein matrix may be estimated by comparison to the small amide rotation rate of 1 s^{-1} (60 min^{-1}) (see above). For Asn-43 and Asn-44, the rotation is quenched by less than 2×10^3 fold and 10^4-fold, respectively. These upper limits are significantly less than the quenching of the average isotopic exchange rates relative to model compounds, 10^6–10^7 and 10^4–10^5 for Asn-43 and Asn-44, respectively.

H_E/H_Z isotopic averaging in this system leads to a new and significant conclusion concerning the dynamic structure of proteins. That is, buried NH_2 groups may rotate rapidly, and their hydrogen bonds break and re-form without exposure to solvent. Breakage and re-formation of NH_2 hydrogen bonds, and C–N rotation, occur many times before a buried $N^{\delta}H$ undergoes hydrogen isotopic exchange with solvent. The NH_2 rotational isomerization may involve transient H bonds to other acceptors as the rotation occurs.

Rapid NH_2 rotational isomerization is particularly remarkable in view of the local environments of Asn-43 and Asn-44 NH_2 groups in folded BPTI [cf. Figures 1 and 10 of Tüchsen and Woodward (1987a)]. Asn-43 NH_2 makes H bonds with two backbone O atoms. Asn-44 H_E makes an H bond to one of the buried waters, which have recently been shown to exchange with solvent waters on a subsecond time scale (Tüchsen et al., 1987). H_Z makes an H bond to the π-system of the Tyr-35 ring. The π-electron cloud on the other side of the Tyr-35 ring also accepts an H bond from the peptide NH of Gly-37. Tyr-35 is known to be relatively immobile with a flip rate of <160 s^{-1} at the temperature used here (Snyder et al., 1975, 1976; Wagner et al., 1976). A relatively small effect of protein tertiary structure on the internal rotation of primary amide groups is most likely a general phenomenon for proteins. Since this is the case for Asn-43, H bonded to three backbone atoms in a very rigid region of a very stable protein, then other buried Asn/Gln primary amide groups are expected to behave similarly.

The magnitude of the upfield shifts of Asn-44 H_Z and Gly-37 NH resonances (Tüchsen & Woodward, 1987a) implies actual interaction of both protons with the Tyr-35 π-system and not mere proximity to the ring. The upfield shifts of Asn-44 H_Z and Gly-37 NH resonances, 4.3 and 3.5 ppm, respectively, are among the largest reported for any protein. Ring current shifts in this range are predicted only if one places the NH group close enough to the ring to give van der Waals overlap of NH and ring atoms (S. J. Perkins, personal communication). These calculations, described in Perkins and Wüthrich (1979) and Perkins (1982), do not take into account electrostatic interactions that may be involved in an NH–π interaction. Although electrostatic contributions must be evaluated before full, quantitative account can be made of the upfield shifts, such contributions also imply NH–π interactions.

The Gly-37–Tyr-35 ring–Asn-44 $N^{\delta}H$ network in BPTI is the first instance of an NH–π interaction between an amide group and an aromatic ring to be shown in proteins. The existence of similar interactions between NH's and π-clouds of secondary amide groups in proteins was predicted and named Hπ–bonds by Basharov et al. (1986) and was suggested by Johanson et al. (1974). The failure of molecular dynamics to account for the experimental free energy barrier of Tyr-35 ring flips (Ghosh & McCammon, 1987) may be because the calculations do not include the Hπ-bonds to Tyr-35.

The question of the relative stability of intramolecular H bonds in proteins is a pivotal point in the discussion of penetration vs local unfolding mechanism of hydrogen exchange (Englander et al., 1980; Hilton et al., 1981; Woodward et al., 1982; Englander & Kallenbach, 1983). Breakage and formation of intramolecular H bonds in proteins on the picosecond time scale are commonly observed in trajectories of molecular dynamics calculations [e.g., Levitt (1983)]. However, an absence of physical evidence in support of easy H-bond breakage was emphasized in Englander and Kallenbach (1983). While the present data do not contain direct information about the time scale of H-bond breakage, they do provide strong experimental evidence that H bonds break and re-form rapidly while buried and without exposure to solvent.

ACKNOWLEDGMENTS

We thank Drs. Stephen Perkins and Raymond Dwek for helpful discussions and advice.

Registry No. BPTI, 9087-70-1; L-Asn, 70-47-3.

REFERENCES

Basharov, M., Val'kenshtein, M., Golovnov, I., Lazarev, Yu., & Sobolev, V. (1986) *Dokl. Akad. Nauk SSSR 287*, 211–215 [*Dokl. Biophys. (Engl. Transl.)* (1986) *27*, 329–332].

Boelens, B., Gros, P., Scheek, R. M., Verpoorte, J. A., & Kaptein, R. (1985) *J. Biomol. Struct. Dyn. 3*, 269–280.

Englander, S. W., & Kallenbach, N. R. (1983) *Q. Rev. Biophys. 16*, 521–655.

Englander, S. W., Calhoun, D., Englander, J., Kallenbach, N., Liem, R., Malin, R., Mandal, C., & Rogero, J. (1980) *Biophys. J. 32*, 577–589.

Ghosh, I., & McCammon, J. A. (1987) *Biophys. J. 51*, 637–641.

Hilton, B., Trudeau, K., & Woodward, C. (1981) *Biochemistry 20*, 4697–4703.

Johanson, A., Kollman, P., Rothenberg, S., & McKelvey, J. (1974) *J. Am. Chem. Soc. 96*, 3794–3880.

Kakuda, Y., & Mueller, D. D. (1974) *Biophys. Chem. 3*, 311–319.

Krishna, N. R., Huang, D. H., Glickson, J. D., Rowan, R., III, & Walter, R. (1979) *Biophys. J. 26*, 345–366.

Krishna, N. R., Sarathy, K. P., Huang, D. H., Stephens, R. L., Glickson, J. D., Smith, C. W., & Walter, R. (1982) *J. Am. Chem. Soc. 104*, 5051–5053.

Levitt, M. (1983) *J. Mol. Biol. 168*, 621–657.

Molday, R. S., Englander, S. W., & Kallen, R. G. (1972) *Biochemistry 11*, 150–158.

Narutis, V. P., & Kopple, K. D. (1983) *Biochemistry 22*, 6233–6239.

Perkins, S. J. (1982) *Biol. Magn. Reson. 2*, 193–336.

Perkins, S. J., & Wüthrich, K. (1979) *Biochim. Biophys. Acta 576*, 409–423.

Perrin, C. L., & Johnston, E. R. (1981) *J. Am. Chem. Soc. 103*, 4697–4703.

Perrin, C. L., Johnston, E. R., Lollo, C. P., & Kobrin, P. A. (1981) *J. Am. Chem. Soc. 103*, 4691–4696.

Redfield, A. G., & Waelder, S. (1979) *J. Am. Chem. Soc. 101*, 6151–6162.

Richarz, R., Sehr, P., Wagner, G., & Wüthrich, K. (1979) *J. Mol. Biol. 130*, 19–30.

Roder, H., Wagner, G., & Wüthrich, K. (1985a) *Biochemistry 24*, 7396–7407.

Roder, H., Wagner, G., & Wüthrich, K. (1985b) *Biochemistry 24*, 7407–7411.

Snyder, G. H., Rowan, R., III, Karplus, S., & Sykes, B. D. (1975) *Biochemistry 14*, 3765–3777.

Snyder, G. H., Rowan, R., III, & Sykes, B. D. (1976) *Biochemistry 15*, 2275–2283.

Tropp, J., & Redfield, A. G. (1980) *J. Am. Chem. Soc. 102*, 534–538.
Tüchsen, E., & Woodward, C. (1985a) *J. Mol. Biol. 185*, 405–419.
Tüchsen, E., & Woodward, C. (1985b) *J. Mol. Biol. 185*, 421–430.
Tüchsen, E., & Woodward, C. (1987a) *Biochemistry 26*, 1918–1925.
Tüchsen, E., & Woodward, C. (1987b) *J. Mol. Biol. 193*, 793–802.
Tüchsen, E., Hayes, J. M., Ramaprasad, S., Copié, V., & Woodward, C. (1987) *Biochemistry 26*, 5163–5172.
Wagner, G. (1980) *Biochem. Biophys. Res. Commun. 97*, 614–620.
Wagner, G., DeMarco, A., & Wüthrich, K. (1976) *Biophys. Struct. Mech. 2*, 139–158.
Wlodawer, A., Walter, J., Huber, R., & Sjölin, L. (1984) *J. Mol. Biol. 180*, 301–329.
Wlodawer, A., Deisenhofer, J., & Huber, R. (1987a) *J. Mol. Biol. 193*, 145–156.
Wlodawer, A., Nachman, J., Gilliard, G., Gallagher, W., & Woodward, C. (1987b) *J. Mol. Biol.* (in press).
Woodward, C., Simon, I., & Tüchsen, E. (1982) *Mol. Cell. Biochem. 48*, 135–160.

Ferreascidin: A Highly Aromatic Protein Containing 3,4-Dihydroxyphenylalanine from the Blood Cells of a Stolidobranch Ascidian†

Lawrence C. Dorsett,‡ Clifford J. Hawkins,*,‡ Janet A. Grice,‡ Martin F. Lavin,§ Pauline M. Merefield,‡ David L. Parry,‡ and Ian L. Ross§

Departments of Chemistry and Biochemistry, University of Queensland, St. Lucia, 4067 Australia

Received March 25, 1987; Revised Manuscript Received August 3, 1987

ABSTRACT: A method of isolation and purification was developed for the major protein from the blood cells of the stolidobranch ascidian *Pyura stolonifera*. The protein, called ferreascidin because of its strong iron binding capacity (two Fe^{3+} per molecule), is the most aromatic protein that has been characterized, with 67% aromatic amino acids including 42% tyrosine and 17% 3,4-dihydroxyphenylalanine. It is a glycoprotein with an apparent sedimentation coefficient of 1.3 S determined by sucrose gradient centrifugation, corresponding to a molecular weight of 10000 which is in agreement with that obtained from sedimentation equilibrium analysis (9800 ± 100). The presence of 3,4-dihydroxyphenylalanine, an amino acid involved in sclerotization of outer body tissues of invertebrates, supports the early proposition that the blood cells are involved in the formation of the test of the ascidian. Circular dichroism of whole cells indicated that the protein was isolated without major structural change.

The chemical constituents of the blood cells of the Ascidiacea, benthic marine invertebrates of the phylum Chordata, have been investigated since early this century (Henze, 1911, 1912). Only one protein has been characterized previously, a protein from the Phlebobranch, *Phallusia mamillata*, known as hemovanadin because of its association with intracellular vanadium (Califano & Caselli, 1948; Henze, 1912; Bielig & Bayer, 1954; Bielig et al., 1966; Boeri & Ehrenberg, 1954; Baltsceffsky & Mendia, 1958; Gilbert et al., 1977).

Endean (1955a) first showed that "morula" blood cells of an ascidian (*Pyura stolonifera*) contain significant concentrations of iron, and more recently, iron has been found generally throughout the Ascidiacea (Swinehart et al., 1974; Biggs & Swinehart, 1976). Research in this laboratory has sought to isolate ligands that bind the iron. This paper reports an unusual protein called ferreascidin that contains 3,4-dihydroxyphenylalanine (DOPA)[1] and has a strong iron binding capacity: it removes a total of two Fe^{3+} ions per molecule of protein from bis(nitrilotriacetato)iron(III) (C. J. Hawkins and Taylor, unpublished results). The catecholate group, a particularly strong chelating group for iron(III), is used by microorganisms to sequester iron (Raymond et al., 1984). DOPA-containing proteins have been shown to possess important functions in invertebrates as extracellular structural proteins (Rainsford, 1967; Degens et al., 1967; Knight & Hunt, 1974; Waite & Anderson, 1978, 1980) and are involved in the attachment of the invertebrates to solid surfaces (Waite & Tanzer, 1980, 1981; Waite, 1986; Mascolo & Waite, 1986; Benedict & Waite, 1986a,b).

Although this is the first report of a DOPA protein from an ascidian or any other chordate, tyrosinase activity has been reported in ascidian embryos (Jeffrey, 1985), and Endean (1955b) has reported the presence of tyrosine-containing proteins in the cells of *P. stolonifera* through staining with Millon's reagent.

Experimental Procedures

Collection of Animals. Specimens of *P. stolonifera* were collected from rocky outcrops below the high-tide level along the shoreline near Hastings Point in northern NSW, and

† This research was supported by grants from the Australian Marine Sciences & Technology Scheme.
‡ Department of Chemistry.
§ Department of Biochemistry.

[1] Abbreviations: CTAB, cetyltrimethylammonium bromide; DOPA, 3,4-dihydroxyphenylalanine; EDTA, disodium ethylenediaminetetraacetate; OPA, *o*-phthalaldehyde; PAGE, polyacrylamide gel electrophoresis; Tris-HCl, tris(hydroxymethyl)aminomethane hydrochloride; SDS, sodium dodecyl sulfate; HPLC, high-performance liquid chromatography; Da, dalton(s).

0006-2960/87/0426-8078$01.50/0